

TIDAL CHARTS OF THE ARABIAN SEA NORTH OF 20° N

KHAWAJA ZAFAR ELAHI AND JURGEN SUNDERMANN

King Saud University, Riyadh, Saudi Arabia

(Received April 10, 1988; revised January 18, 1989)

A depth-averaged two-dimensional numerical model (20° N to 25° N, 56° E to 70° E) of the Arabian sea is developed to reproduce the major diurnal and semi-diurnal tidal constituents. The model has a resolution of 1/2° both latitude and longitude and has open boundaries at latitude 20° N and in the strait of Hormuz at longitude 56°. 22'E. The boundary conditions on the open boundaries are derived from the empirical co-amplitude and co-tidal charts of the Arabian sea.

The classical non-linear hyperbolic initial and boundary value problem of long wave propagation in shallow waters is solved by the explicit finite difference technique. The results regarding tidal elevation are used to develop detailed co-amplitude and co-tidal charts for principal tides. These charts make it possible to predict the tidal elevation at the coast and in the open sea area with greater accuracy.

Key Words: Tide, Numerical model, Arabian Sea.

Introduction

The depth values of the Arabian Sea north of 20°N are compiled from the chart No. INT 705 edited by the Deutsches Hydrographisches Institute. Depth contours are shown in Fig. 1. Pakistan Coastal waters, the Indus Delta, Gulf of Kutch and Strait of Hormuz are very shallow with average water depth of 30 meters. 200 meters depth, which slopes into deep water, is in range of 10 to 30 km from the Omani Coast, 30 to 50 km from Iranian and Southern Pakistani Coasts, 100 to 500 km from Bay of Somiani and Diu Head. Coastal area from Muskat to Masiriah are deeper than the rest of the coastal areas. Maximum water depth of 4259 meters occurs near the Murray Ridge.

Tidal charts can be prepared either using the information available in the form of analyses of long and short sets of observations of waterlevel fluctuations on the coastal gauges or using numerical models. The information available about tides in the Arabian sea will be summarized below.

McCommon and Wunsch [4] constructed charts for the major semi-diurnal and diurnal tidal constituents of the Indian Ocean north of 15° S. Co-amplitude and co-tidal lines in these charts are drawn on the basis of the analysed coastal tidal observational data. Fairbairn (1954) prepared a tidal chart of K_2 - tide using Proudman's Theorem. Bogdanov and Karkov [1] were the first to develop a mathematical model to analyse the tidal phenomena in the Indian Ocean. A small amount of

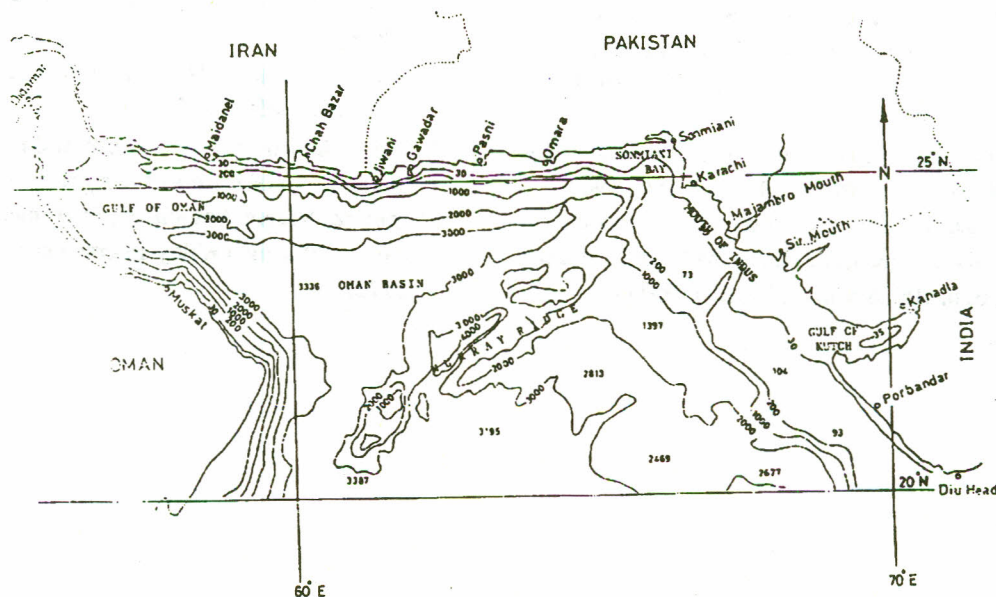


Fig. 1. Bathymetry of the Northern Arabian Sea.

information is also available from mathematical model of the world ocean [6,7,10,11]. In the existing tidal charts, consideration is mainly given to the position of the amphidromic system. A little information is provided about amplitude variation in the Arabian Sea but there is no information about the tidal variation in the area.

The numerical model consists of the Navier-Stokes equation and equation of continuity. These equations are solved with the explicit finite-difference technique. These include the effects of bottom friction, rotation of earth and atmospheric pressure gradient.

In the present paper detailed pictures of amplitude and phase distributions in the area are compiled for four major tidal constituents. The resolution of the co-amplitude lines is 2 cm for the M_2 -tide, 1 cm for S_2 -, K_1 -tide. The successive difference in co-tidal lines is 1 for all four partial tides.

The accuracy of the computed tidal charts depends upon the quality of values of the prescribed water level or velocity on the open boundaries. Open boundary is a supposed joining line between the modelled area and the main sea.

Value of water level on the open boundaries obtained through the values on the coastal gauges did not produce accurate results. Thus, the tidal charts for M_2 -, S_2 -, K_1 - and O_1 - tide (Figs. 2-5) were prepared on the basis of extrapolation of observed values in the Tide Tables, DH1 1973, IFM 1973, PAK 1978, and the world tidal charts. These charts were used to access values of water level on the open boundaries.

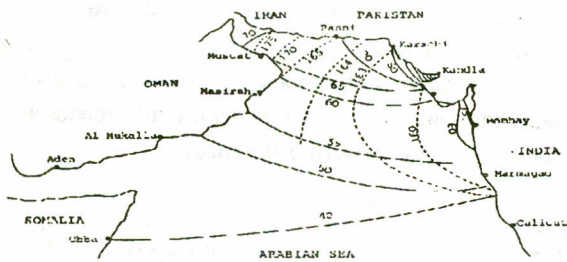


Fig. 2. M_2 -tide in the Arabian Sea.
Co-amplitude lines in cm (full)
Co-tidal lines in degree related to Greenwich (broken)

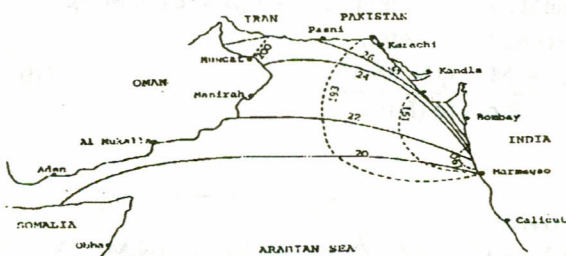


Fig. 3. S_2 -tide in the Arabian Sea
Co-amplitude lines in cm (full)
Co-tidal lines in degree related to Greenwich (broken)

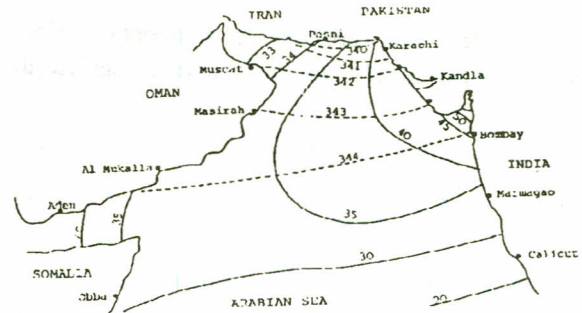


Fig. 4. K_1 -tide in the Arabian Sea
Co-amplitude lines in cm (full)
Co-tidal lines in degree related to Greenwich (broken)

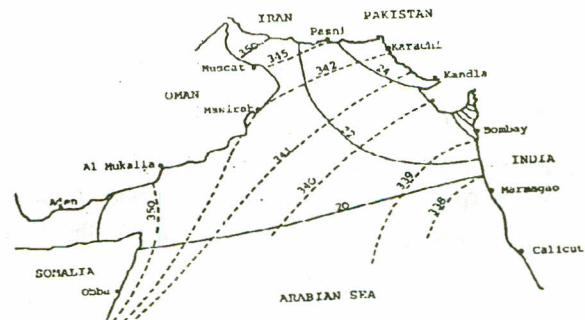


Fig. 5. S_2 -tide in the Arabian Sea
Co-amplitude lines in cm (full)
Co-tidal lines in degree related to Greenwich (broken)

Numerical computations were made with model closed at the Strait of Hormuz. Tides having high amplitudes were produced, due to converging geometry. Co-tidal values were out of phase due to superposition of reflecting wave. Tides are reproduced more accurately by considering an open boundary between the Arabian Gulf and the Arabian Sea at the strait of Hormuz.

Mathematical model of the northern Arabian sea: The system of equations which describes the tidal dynamics of large fluid masses is derived from hydrodynamic equations of motion and continuity. The water level variation as a function of time is prescribed on the open boundaries in place of a tide generating force. Since water movements are mainly horizontal and the horizontal dimensions are much greater than the depth, the system of equations has been simplified to a two-dimensional system in the model. Effect of the Earth's curvature is taken into account by considering the depth averaged equations of motion and continuity in spherical polar co-ordinates as follows:

$$\frac{\partial \zeta}{\partial t} + \frac{1}{R \cos \phi} \left[\frac{\partial (HU)}{\partial \lambda} + \frac{\partial (HV \cos \phi)}{\partial \phi} \right] = 0 \quad (1)$$

$$\frac{\partial U}{\partial t} - 2 \omega \sin \phi V + \frac{1}{H} \tau_b^\lambda - A_h \nabla^2 U + \frac{g}{R \cos \phi} \frac{\partial \zeta}{\partial \lambda} = 0 \quad (2)$$

$$\frac{\partial V}{\partial t} - 2 \omega \sin \phi U + \frac{1}{H} \tau_b^\phi - A_h \nabla^2 V + \frac{1}{R} \frac{\partial \zeta}{\partial \phi} = 0 \quad (3)$$

If $u(z)$ and $v(z)$ denote the horizontal velocity components at depth z below the undisturbed sea surface, then

$$U = \frac{1}{h + \zeta} \int_{-\zeta}^{\zeta} u(z) dz \quad (4)$$

$$V = \frac{1}{h + \zeta} \int_{-\zeta}^{\zeta} v(z) dz \quad (5)$$

The stresses due to roughness of the bottom (τ_b^x, τ_b^y) are parameterized empirically using the Newton-Taylor formulation, (G.I. Taylor, 1919), which is a quadratic law relating bottom stress to the depth mean current.

$$\tau_b^x = rH^{-1} U(U^2 + V^2)^{1/2} \quad (6)$$

$$\tau_b^y = rH^{-1} V(U^2 + V^2)^{1/2} \quad (7)$$

in which $r = .003$ is the bottom friction co-efficient.

The coefficient of horizontal eddy viscosity is related to grid size and time step of the numerical model by the relation:

$$A_h = \frac{1 - \alpha \Delta t}{4} \frac{\Delta l}{\Delta t} \quad (8)$$

α takes value between 0.90 and 0.99, depending upon the inner viscosity of the fluid (Sundermann, 1966). Through numerical experimentation, its numerical value is estimated 0.99 in shallow water areas and 0.9 in deep water areas. The value of $\alpha = .99$ in Eq. (8) is taken due to the fact of low depth off the Karachi and Western Indian coast.

The following notations have been used:

- U, V components of vertically averaged velocity in the λ and ϕ directions, resp. [m/s].
 ζ water elevation [m]
 A_h horizontal eddy coefficient [m²/s]
 g acceleration due to gravity [m²/s]
 h mean water depth [m]
 $H = h +$ actual depth [m]
 r bottom friction coefficient
 R Radius of the Earth [m]
 t time [s]
 λ, ϕ geographical longitude and latitude
 ω angular velocity of the Earth's rotation [1/S]
 ∇^2 horizontal Laplacean operator [1/m²]

The tides in the Arabian Sea are supported predominantly by the semidiurnal constituents M_2 and S_2 with small contributions from the diurnal constituents K_1 and O_1 . The tide in the model is generated by prescribing amplitudes and phases of tidal constituents at open boundaries, Waterlevels as a function of time for 4 main tidal constituents, M_2, S_2, K_1 and O_1 are supposed to be known and calculated by.

$$\zeta(t) = A \cos(\sigma t - \kappa) \quad (9)$$

where A is amplitude, κ is phase of incoming tide and σ is frequency

TABLE 1: PARTIAL TIDES AND THEIR FREQUENCIES

Partial tide	σ frequency, 10 ⁻⁴ /S
Semi-diurnal	
M_2 Principal lunar	1.40519
S_2 Principal solar	1.45444
Diurnal	
K_1 Lunar-solar	0.72921
O_1 Principal lunar	0.67598

Initial and boundary conditions: The solution of the above equations require the knowledge of boundary and initial conditions. There are two types of boundary conditions.

1. Solid boundary (coastline)

$$u = v = 0 \text{ no-slip condition}$$

2. Open boundary

Water elevations are prescribed at every time step by using Eq.(9). Moreover, the velocity gradients in the normal direction are zero.

$$\frac{\partial V}{\partial n} = 0$$

As initial condition the values of water elevation and velocity are taken to be zero at $t = 0$.

Finite difference formation: The system of partial differential equations (1-3) with the initial and boundary conditions is transferred into a set of algebraic equations by replacing the space derivatives by central differences and the time derivatives by forward differences.

$$U(N, M) = (1 - r \Delta t) \sqrt{\frac{(t)}{H U(N, M)^2 + V_u^{(t)}(N, M)^2}} U(N, M) + \frac{2\omega \Delta t \sin(\phi(N)) V u^{(t)}(N, M) + A_h \Delta t \nabla^2 U(N, M) + g \Delta t}{(t + \Delta t/2)} \frac{\zeta(N, M) - \zeta(N, M+1)}{R \cos(\phi(N))} \quad (10)$$

$$V(N, M) = (1 - r \Delta t) \sqrt{\frac{(t)}{H V(N, M)^2 + U_u^{(t)}(N, M)^2}} V(N, M) - \frac{2\omega \Delta t \sin(\phi(N)) U v^{(t)}(N, M) + A_h \Delta t \nabla^2 V(N, M) - g \Delta t}{(t)}$$

$$\frac{\zeta(N, M) - \zeta(N+1, M)}{R\Delta\phi} \quad (11)$$

$$\zeta(N, M) = \zeta(N, M) + \frac{\Delta t}{R\cos(\phi(N))} \frac{(HU(N, M) U(N, M) - HU(N, M-1) U(N, M-1) - HV(N, M) V(N, M) \cos(\phi(N)) - HV(N-1, M) V(N-1, M) \cos(\phi(N-1)))}{\Delta\lambda} \quad (12)$$

where

$$HU(N, M) = hU(N, M) + \frac{1}{2} (\zeta(N, M) + \zeta(N, M+1)) \quad (13)$$

$$HV(N, M) = hV(N, M) + \frac{1}{2} (\zeta(N, M) + \zeta(N, M+1)) \quad (14)$$

$$U_v(N, M) = \frac{1}{4} (U(N, M-1) + U(N, M) + U(N+1, M-1) + U(N+1, M)) \quad (15)$$

$$U_v(N, M) = \frac{1}{4} (V(N, M-1) + V(N, M) + V(N-1, M+1) + V(N-1, M)) \quad (16)$$

$$\nabla^2 U \approx \frac{1}{\Delta l^2} (U(N-1, M) + U(N+1, M+1) + U(N, M+1) + U(N, M-1)) \quad (17)$$

$$\nabla^2 V \approx \frac{1}{\Delta l^2} (V(N-1, M) + V(N+1, M) + V(N, M+1) + V(N, M-1)) \quad (18)$$

Where

$$\Delta l = R\Delta\phi$$

For this method efficient time step is required for numerical stability and is obtained by using the Courant-Friedriches-Lewy stability condition (Neumann and Richtmyer 1950). The maximum time step be chosen so that any combination of signals can transverse at most one zone per time step [$t = 150 \text{ sec}$], mathematically, it is interpreted as

$$\Delta t \leq \frac{1}{\sqrt{2gh_{\max}}} \quad (19)$$

where l is the grid isze and h_{\max} is maximum water depth in the area.

Results

The grid distance of 0.5° (Fig. 6), time interval of 150 seconds, frictional coefficient r of 3×10^{-3} and horizontal eddy viscosity A_h of $.1 \times 10^6 \text{ m}^2/\text{sec}$ are chosen for calculating the tidal phenomena at 12×30 computational points in the northern Arabian Sea.

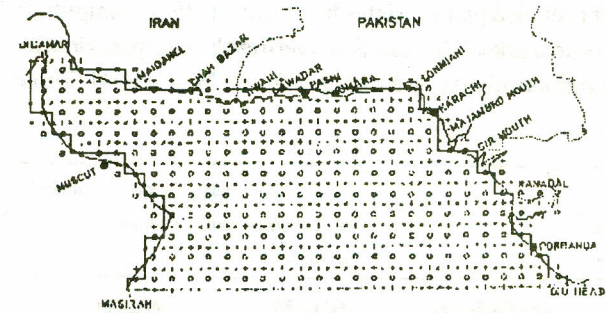


Fig. 6. Finite-difference grid for the Northern Arabian Sea
 + computational point for ζ
 x computational point for u
 • computational point for v
 ● tidal gauge

The set of explicit finite differs equations (10-18) have been evaluated numerically using the hydrodynamical-numerical method (Hansen 1956) by means of computer program written in FORTRAN IV. The computational work was done on a CDC 7600 computer at Technical University, Hannover (W. Germany). The numerical solutions converged after 10 tidal cycles in the case of the semi-diurnal tides and 5 tidal cycles in the case of diurnal tides.

Schwiderski (1980) developed a numerical model for the principal tidal constituents over the globe as a whole with the space resolution of $1^\circ \times 1^\circ$. The results of the model cannot be used for the comparison because the initial values are hydrodynamically interpolated values of the coastal gauges and these values are found not accurate. For M2- tide comparison between the initial values used by Schwiderski and observed value at the Karachi and Porbandar is given in Table 2.

TABLE - 2

PLACE		Schwiderski	Observed
Karachi	amplitude (cm)	81	79.8
	phase (deg)	185	163.7
Porbandar	amplitude (cm)	68	65
	phase (deg)	180	187

McCommon and Wunsch [4] prepared empirical charts of the principal tidal constituents in the northern part of the Indian Ocean north of 15° S . Charts were drawn on basis of the

Indian Ocean north of 15 S. Charts were drawn on basis of the observational data on coastal gauges and some deep sea records. In those regions where essentially no data was available interpolation was made. The information on these charts about tidal variation is summarised and is used for comparison.

Tidal charts of the Arabian Sea north of 20° N for M_2 -tide, S_2 -tide, K_1 -tide and O_1 -tide are shown in Figs. 7-10. These present detailed picture of the distribution of the co-amplitude and co-tidal lines. The results are verified by comparison with observational charts by McCommon and Wunsch [4] (Table 3).

TABLE 3

Tidal Constituents	Observation chart	Numerical model
	McCommon and Wunsch	Charts
M_2	amplitude cm	60 to 80
	phase (deg)	150° to 180°
S_2	amplitude cm	20 to 30
	phase (deg)	180° to 210°
k_1	amplitude cm	30
	phase (deg)	330° to 359°
O_1	amplitude cm	20 to 25
	phase (deg)	330° to 359°

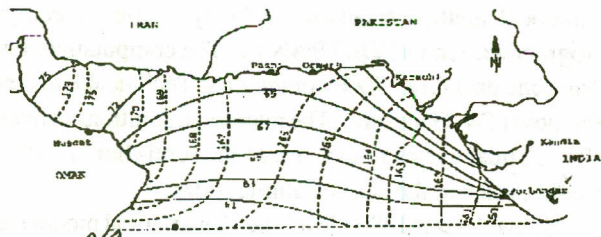


Fig. 7. M_2 -tidal in the Northern Arabian Sea. Co-amplitude lines in cm (full). Co-tidal lines in degree related to Greenwich (broken)

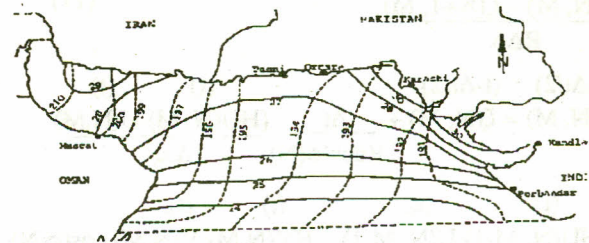


Fig. 8. S_2 -tidal in the Northern Arabian Sea. Co-amplitude lines in cm (full). Co-tidal lines in degree related to Greenwich (broken)

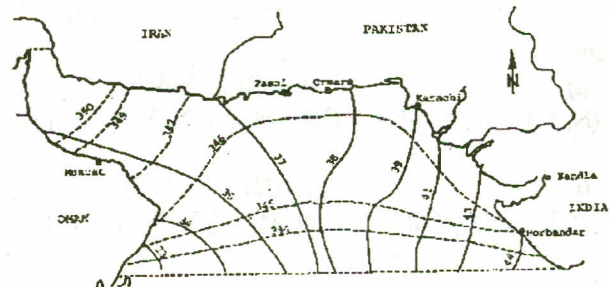


Fig. 9. K_1 -tidal in the Northern Arabian Sea. Co-amplitude lines in cm (full). Co-tidal lines in degree related to Greenwich (broken)

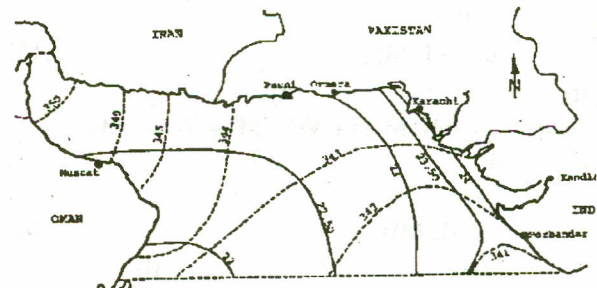


Fig. 10. O_1 -tidal in the Northern Arabian Sea. Co-amplitude lines in cm (full). Co-tidal lines in degree related to Greenwich (broken)

TABLE 4. COMPUTED (C), OBSERVED (O), AMPLITUDE (A) AND PHASE(K) OF THE MAJOR TIDAL CONSTITUENTS.

Tidal constituent	Site	a (cm)	M_2		S_2		K_1		O_1	
			c	o	c	o	c	o	c	o
Porbandar	a	67,92	65,0	27,57	24,0	45,17	46,0	24,11	24,0	
	k	161,43	157,0	191,51	220,0	345,89	336,0	342,10	342,0	
Karachi	a	79,91	79,8	31,47	29,6	39,22	41,1	23,68	20,0	
	k	166,34	163,7	194,67	193,9	347,51	342,2	343,93	343,2	
Omara	a	69,54	70,0	27,27	24,0	37,72	43,0	22,94	18,0	
	k	166,29	156,1	194,24	176,0	346,47	340	343,68	343,3	
Pasni	a	68,98	69,0	27,07	26,0	37,38	31,0	22,91	24,0	
	k	166,37	165,0	194,48	192,0	346,42	346,0	343,79	346,2	
Muscat	a	69,75	63,3	27,27	23,7	35,99	38,8	22,48	20,2	
	k	171,74	159,8	199,33	189,8	347,76	341,4	345,71	342,4	

TABLE 5 AMPLITUDE A (CM), PHASE K (DEG), WATERLEVEL AT T=0 AND AT T=T/4, ζ_1 AND ζ_2 (CM); T TIDAL PERIOD

No. location	geograph. pos.		M2	S2	K1	O1	
	N	E					
Pakistan							
1. Sir Mouth	23°56'	68°12'	a	77.15	30.22	39.83	23.53
			k	165.37	193.83	347.99	343.59
			ζ_1	-74.65	-29.40	38.96	22.57
2. Majarhro Mouth	24°10'	67°32'	ζ_2	19.49	-7.15	-8.29	-6.63
			a	77.50	30.48	39.82	23.57
			k	166.34	194.03	347.37	343.66
3. Karachi	24°82'	66°37'	ζ_1	-75.31	-29.57	38.33	22.62
			ζ_2	18.31	-7.39	-8.59	-6.65
			a	79.91	31.42	39.22	23.68
4. West point	25°24'	66°31'	k	167.32	194.67	347.51	343.93
			ζ_1	-77.97	-30.44	38.23	22.75
			ζ_2	17.54	-7.97	-8.84	-6.55
5. Omara	25°11'	64°41'	a	79.91	31.47	39.22	23.68
			k	168.66	196.18	347.75	344.51
			ζ_1	-77.59	-29.89	38.22	22.80
6. Pasni	25°20'	63°50'	ζ_2	15.56	-8.67	-8.30	-6.32
			a	69.54	27.27	37.72	22.94
			k	166.29	194.24	346.47	343.68
7. Gawadar	25°11'	62°33'	ζ_1	-67.55	-26.43	36.67	22.06
			ζ_2	16.48	-6.71	-8.82	-6.46
			a	68.98	27.07	37.38	22.91
8. Jiwani	25°06'	61°83'	k	166.37	194.48	346.42	343.79
			ζ_1	-67.07	-26.21	36.34	22.00
			ζ_2	16.10	-6.77	-8.78	-6.39
9. Chah Bazar	25°30'	60°70'	a	69.12	27.16	37.11	22.86
			k	166.95	194.99	346.47	344.00
			ζ_1	-67.33	-25.23	36.08	21.96
10. Maidanel	25°40'	59°20'	ζ_2	15.61	-7.03	-8.68	-6.30
			a	69.41	27.28	37.02	22.87
			k	167.22	195.31	346.55	344.13
11. Muscat	23°62'	58°60'	ζ_1	-67.69	-26.31	36.00	22.00
			ζ_2	15.36	-7.20	-8.61	-6.25
			a	70.68	29.75	36.81	22.92
12. Rasal Hadd	23°55'	59°80'	k	168.79	197.06	347.08	344.81
			ζ_1	-69.33	-26.53	35.88	22.09
			ζ_2	13.74	-8.14	-8.23	-6.00
13. Porbandar	21°63'	69°62'	a	73.24	28.60	36.84	23.04
			k	171.06	199.61	348.25	345.87
			ζ_1	-72.35	-26.94	36.06	22.34
India	21°63'	69°62'	ζ_2	11.39	-9.60	-7.50	-5.62
			a	68.75	27.27	35.99	22.48
			k	171.14	199.33	347.76	345.79
13. Porbandar	21°63'	69°62'	ζ_1	-68.92	-25.73	35.18	21.80
			ζ_2	10.75	-9.03	-7.63	-5.52
			a	65.79	25.84	35.56	22.19
13. Porbandar	21°63'	69°62'	k	169.06	197.08	346.50	344.81
			ζ_1	-64.60	-24.70	34.58	22.95
			ζ_2	12.49	-7.59	-8.30	-5.82
13. Porbandar	21°63'	69°62'	a	67.92	27.57	45.17	24.11
			k	161.43	191.51	345.89	342.10
			ζ_1	-64.38	-27.02	43.61	21.41
13. Porbandar	21°63'	69°62'	ζ_2	21.63	-5.50	-11.01	-7.41

The results of the numerical model are also being compared with the available observational values at the coastal tidal gauges; Porbandar, Karachi, Ormara, Pasni and Muscat (Table 4). The computed values are in good agreement with the observed values. The deviation of the computed values from the observed harmonic constants at the gauge Omara might be due to local effects. The increase in phase by 12° and amplitude by 6 cm for M2-tide at the gauge Muscat is due to the reason that this gauge is under influence of two open boundaries.

The harmonic constants for four major tides at 13 important places on the coast of the northern Arabian Sea are presented on basis of the numerical model (Table 5).

Conclusion

The tidal charts prepared with the help of the hydrodynamical-numerical model had a high level of accuracy. They present a detailed picture of the amplitude and phase distribution and hence give the structure of the tidal wave of given frequency. These may be used to provide the necessary boundary values at the open boundary for a numerical model of the near shore area and also used to control the results of the model. The accuracy of the results of short sets of observation at a temporary tidal gauges may be checked with the help of these charts.

References

1. K.T. Bogdanov, and B.V. Karkov, *Ocnology*, **15**, 1975.
2. Elahi, Kh. Z., Berechnung von lokalen Gezeitenphänomenen in einem Gebiet mit geringem Beobachtungsmaterial mit Anwendung auf die Sonmiani Bucht, Mitt. des Franzius-Instituts für Wasserbau und Küsteningenieurwesen der Tech. Univ. Hannover, Nr., 48 (1978).
3. W. Hansen, Theorie zur Errechnung des Wasserstandes und der Stromungen in Randmeeren nbst Anwendungen, *Tellus* 8, Nr. 3 (1956).
4. C. McCommon and C. Wunsch, *J. Geophys. Res.*, **82**(37)(1977).
5. J.V. Neumann, R.D. Richtmyer, *J. Appl. Physics*, **21**(1950).
6. C.L. Pekeris, and V. Accad, *Phil. Trans. Roy. Soc. London, Ser. A* (1969).
7. E.W. Schwinderski, *Rev. of Geoph. and Sp. Phy.*, **18**(1), 243(1980).
8. J. Sundermann, Ein Vergleich der analytischen und numerischen Berechnung winderzevgtter Stromungen and wasserstande in einem Modellmeer mit Anwendungen auf die Nordsee, *Mitteilungen des Inst. für Meerskunde der Universität Hamburg. IV* (1966).

10. W. Zahel, Die Reproduktion gezeitenbedingter Bewegungsvorgänge im Weltozean mittels des hydrodynamisch-numerischen Verfahrens, Mitt. d. Inst. f. Merreskunde d. Univ. Hamburg, XVII (1970).
11. W. Zahel, Pure Appl. Geoph., 109 (1973).
12. Deutsches Hydrographisches Institut (DHI), Gezeitentafeln für die Jahre, Band II, DHI, Hamburg 1968, 1973.
13. The Hydrographic Department Pakistan Navy (PAK), Tide Tables for Pakistan Ports, PAK, Karachi, 1978.
14. Institut für Meereskunde (IfM), Gezeitentafeln für den Weltozean, Hamburg, 1973 (unpublished).